Figure S1. The catalytic module residues involved in the interaction between INCENP and aurora kinase B proteins are conserved in *T. gondii* CPC complex. (A). Structural organization of the localization module (centromere and spindle targeting motifs; borealin and survivin binding domain) of HsINCENP, of its coiled-coil domain (CC) and of its catalytic module (IN-box motif known to interact with the N-lobe of aurora kinase B). Motif and domain prediction programs and sequence alignments did not allow us to identify with certainty the interaction domains with centromeres, mitotic spindle, and borealin and survivin proteins. Only the IN-box motif was found without certainty in both *T. gondii* INCENPs. HP1: heterochromatin protein. **(B and C).** Sequence alignment of the INCENP IN-box or Aurora kinase B N-lobe in several model organisms. Residues highlighted in blue or pink represent key residues involved in the interaction between INCENP and Aurora kinase B proteins. Conserved residues are colored in grey. (.) represents conserved residues; (:) represents similar residues; (*) represents identical residues.

Figure S2. Epitope tagging of TgArk1 and its controlled expression by shield-1. (A). Schematic representation of the primary structure of TgArk1 Aurora kinase 1 protein highlighting its kinase domain; the kinase domain have been searched with SMART (http://smart.embl-heidelberg.de). The kinase domain of TgArk1 is highlighted in pink. **(B).** Scheme illustrating the approach used to endogenously tag TgArk1 at the N-terminus end in RH-Δku80 using CRISPR/Cas9 nuclease mediated gene recombination strategy. To induce a double strand break 13 base pair just downstream the start codon of Ark1 (black) and introduce a HA_3-tag by double homologous recombination, a cas9-Ark1 gRNA expression plasmid (pU6-HA_3Tag) was transfected together with a linear 500 bp donor DNA fragment containing Ark1 homology regions for double strand break repair. Recodonized DNA sequence of the donor fragment is hatched. **(C).** Schematic representation of Ark1WT or Ark1D338A fused to DD

and Myc tag. In absence of shield-1 the proteins will be degraded in the proteasome. In contrast, adding the shield-1 to the culture medium will trigger the stabilization of both proteins. **(D).** Immunofluorescence assays performed on transgenic parasites expressing DD-Myc-Ark1WT or DD-Myc-Ark1D/A proteins using anti-myc antibodies. Parasites were grown in presence of Shld-1 for 12 hours before fixation and staining with anti-myc antibodies. Scale bars represent 2 μm.

Figure S3. (A). ***TgChromo1, TgCEP250L1*** **and** ***TgBub3*** **endogenous epitopes tagging.** Insertion of three HA-epitope tags at the C-termini of TgChromo1, TgCEP250L1 and TgBub3 by single homologous recombination at the 3' of the corresponding gene (knock-in).

Figure S4. TgArk1 is involved in the formation of a regular number of daughter cells within a mother cell and is important for the biogenesis of IMC. (A). IFA of representative ark1D/A-Δku80 vacuole untreated with shield-1 (upper panel) which was compared with IFA to two representative ark1D/A-Δku80 vacuoles cultured in presence of shield-1 (lower panels). As depicted in the upper vacuole containing 4 parasites, two regular daughter cells are formed within each mother cell (green staining). In contrast, in both vacuoles treated with shield-1 for 12 hrs, the formation of IMC buds is irregular (> 2, yellow arrows) and does not appear in all parasites. Anti-GAP45 (in red) and anti-ISP1 (in green) antibodies, respectively, were used to detect the pellicle and nascent buds. Scale bars represent 2 μm. **(B).** Intracellular growth assay of indicated parasite strains (RH-Δku80, ark1WT-Δku80 and ark1D/A-Δku80). Replication was analyzed in presence or in absence of Shld-1 after 12 hours of treatment. Values are means ± SD for three independent experiments. **(C).** Stabilization of DD-Myc-Ark1D/A protein leads to collapse of the IMC. While untreated parasites showed normal IMC organelle surrounding each parasite (first panel on the left, red staining), parasites expressing DD-Myc-Ark1D/A protein

in presence of shield-1 displayed defects in the formation of their IMCs (middle panel and last panel on the right, green arrows). Gaps were visualized by IFAs using anti-IMC1 antibodies indicating defects in IMC biogenesis. Scale bars represent 2 μm.

Figure S5. Examination of TgINCENP1 localization during tachyzoite replication, and studying its interaction with TgArk1. (A). *TgINCENP1* endogenous epitope tagging. Insertion of a GFP or three HA-epitope tags at the C-terminus of TgINCENP1 by single homologous recombination at the 3' end of the gene (knock-in). **(B).** Immunofluorescence images reveal that TgINCENP1 is exclusively found in the nucleus in non-dividing parasites. Parasites were co-stained with antibodies for INCENP1-HA_3 and IMC1 as well as stained with DAPI. Representative images at 2 cell cycle phases are shown as identified by established cell cycle criteria based on the absence or presence of internal daughters (red = IMC1). Scale bars represent 2 μm. **(C).** The endogenous protein TgINCENP1 and TgArk1 were fused to a GFP and Myc tags, respectively (2^{nd} line). GFP protein alone and TgArk1 protein fused to a Myc tag was used as negative control (1^{st} line). Pull-down experiments were carried out using the GFP-Trap system. Proteins that bind to GFP or to TgINCENP1-GFP were eluted and subjected to western blot analysis with anti-GFP (left lanes) and anti-Myc (right lanes) antibodies.

Figure S6. TgINCENP1 conditional knock-in by promoter exchange strategy and regulation of TgINCENP1i-HA_3-Expressing Parasites. (A). Schematic representation of the strategy used to replace the endogenous promoters of TgINCENP1 with the tetracycline inducible promoter. The DHFR-tetO7-Sag4-NtgINCENP1 plasmid contains the dihydrofolate reductase (DHFR) gene (in yellow) and the N-terminus genomic coding sequence of TgINCENP1 (in grey) under the control of the inducible tetO7Sag4 promoter (orange arrow). Black arrows represent the primers used for PCR analysis and the length of the PCR fragments

generated is indicated. To study the regulation of TgINCENP1i gene, we inserted by single homologous recombination at the 3' end of the gene, a sequence coding for three HA epitope tags (in blue) at the C-terminus of the corresponding TgINCENP1i protein. **(B).** PCR analysis performed on Tgincenp1i, showing that single homologous recombination occurred. Genomic DNA from TATi1-Δku80 parasites was used as negative control. **(C).** Down-regulation of TgINCENP1i-HA_3 in the incenp1i strain as shown by IFA with anti-HA antibodies 2 days after ATc treatment (lower panel). Anti-IMC1 antibodies were used to visualize the mother and daughter parasites. Under the control of Sag4 promoter, TgINCENP1i-HA_3 protein is expressed constitutively during the different phases of the parasite cell cycle and is found dispersed in the cytoplasm as well as in the nucleus. The nuclei were stained with DAPI. Scale bars represent 2µm. **(D).** Western blot analysis of TgINCENP1-HA_3 and TgINCENP1i-HA_3 (± ATc) strains. TgINCENP1i-HA_3 parasites were treated for 2 days with ATc. SAG1 was used as loading control.

Figure S7. Phenotypic analysis of TgINCENP1-depleted parasites. (A). Plaque assay stained with Giemsa 7 days after invasion of the host cells with wild-type TATi1-Δku80 and incenp1i strains. **(B).** Intracellular growth assay performed by counting the numbers of parasites per vacuole (x-axis) 24 hours after invasion of the host cells. The percentages of vacuoles containing varying numbers of parasites are represented on the y-axis. Values are means ± SD for three independent experiments. **(C).** Endodyogeny assay performed on TATi1-Δku80 or incenp1i strains cultivated in presence or absence of ATc for 48 hours and allowed to invade new HFF cells. Numbers of vacuoles showing the formation of newly formed buds (y-axis) were counted 24 hours after inoculation using anti-ISP1 antibodies. Values are means ± SD for three independent experiments. **(D).** Immunofluorescence assays of HA_3-Ark1 in intracellular incenp1i parasites grown without or in the presence of ATc for 3 days. Endogenous TgArk1

was detected using anti-HA antibodies. The parasite anterior part was visualized using anti-AMA1 antibodies. Nuclei were stained with DAPI. Scale bars represent 2μm.

Figure S8. Expression and localization of TgINCENP2 in tachyzoites. (A). Insertion of Myc tag at the N-terminus of TgINCENP2 and promoter exchange by single-homologous recombination at the 5′ of the gene (knock-in in RH-Δku80 strain). gNt, genomic N-terminal. **(B).** Immunofluorescence images reveal that TgINCENP2 can switch from nucleus to cytoplasm depending on phase during parasite division. Parasites were co-stained with antibodies for Myc-INCENP2 and IMC1 as well as stained with DAPI. Representative images at 2 cell cycle phases and transitions are shown as identified by established cell cycle criteria based on nuclear morphology (DAPI, single or U-shaped), and the presence of internal daughters (red = IMC1). Scale bars represent 2 μm. **(C).** Western blot analysis performed on transgenic or RH-Δku80 parasite lysates probed with anti-Myc antibodies. Myc-TgINCENP2 is found at the expected molecular mass (143 kDa).

Figure S9. TgINCENP2 knock-down by inserting the 7 repeats of the tetracycline operon upstream of the endogenous promoter of the *INCENP2* gene. (A). Scheme illustrating the approach used to generate incenp2i strain in TATi1-Δku80 using CRISPR/Cas9 nuclease mediated gene recombination strategy. To induce a double strand break 1084 bp just downstream the endogenous promoter (in blue) of INCENP2 (black) and introduce the DHFR resistance cassette (in grey) and the tetO7 sequence (in yellow) by double homologous recombination, a cas9-INCENP2i gRNA plasmid (pU6-INCENP2i) was transfected together with a linear 3002 bp donor DNA fragment containing INCENP2 homology regions for double strand break repair. The primers used for PCR analysis are indicated by black arrows and the length of the PCR fragments is specified. **(B).** PCR analysis performed on incenp2i, showing

that double-homologous recombination had occurred. Genomic DNA from TATi1-Δku80 parasites was used as negative control. **(C).** Semi-quantitative RT-PCR analysis of TgINCENP2 expression in the wild-type and mutant parasites, preceded or not by 1 day of ATc treatment to regulate expression. The FYVE1 gene was used as a loading control.

Figure S10. TgINCENP2 is essential for nucleus segregation and for the duplication of key subcellular structures associated to mitosis. (A). Quantification of the number of nucleus-deficient parasites in two different strains (TATi1-Δku80 and incenp2i) in the presence or absence of ATc for 24 hours. The percentage of parasites displaying nucleus segregation defect was determined for at least 300 parasites. The results shown are from three independent experiments. **(B).** Quantification of the number of vacuoles showing nuclei in residual bodies in two different strains (TATi1-Δku80 and incenp2i) ± ATc for 24 hours. At least 300 vacuoles were examined for each condition. Values are means ± SD for three independent experiments. **(C and D).** Quantification of the number of parasites showing a stretched centrosome inner core or spindle pole in two different strains (TATi1-Δku80 and incenp2i) in the presence or absence of ATc for 24 hours. At least 300 parasites were examined for each condition. Values are means ± SD for three independent experiments. **(E and F).** The average of TgCEP250L1-HA_3 containing centrosomes inner cores or TgEB1-YFP containing spindle poles per parasite, was quantified in 300 parasites revealing a significant reduction of the spindle poles and centrosomes inner cores when incenp2i parasites were treated in presence of ATc for 24 hours. Values are means ± SD for three independent experiments. **(G and H).** Quantification of the number of parasites showing a stretched kinetochore or centromere in two different strains (TATi1-Δku80 and incenp2i) in the presence or absence of ATc for 24 hours. At least 300 parasites were examined for each condition. Values are means ± SD for three independent experiments. **(I).** The average of TgNDC80 containing kinetochores per parasite was quantified

in 300 parasites revealing a significant reduction of the kinetochores when incenp2i parasites were treated in presence of ATc for 24 hours. Values are means ± SD for three independent experiments.

Figure S11. TgINCENP2 is essential for centromere duplication, kinetochore/centromere clustering, proper duplication of the centrosome outer core, centrosome outer core/kinetochore pairing and for parasite replication. (A). The average of TgChromo1 containing centromeres per parasite was quantified in 300 parasites revealing a significant reduction of the centromeres when incenp2i parasites were treated in presence of ATc for 24 hours. Values are means ± SD for three independent experiments. **(B).** Quantification of the number of parasites showing clustered or detached kinetochore/centromere pairing in two different strains (TATi1-Δku80 and incenp2i) in the presence or absence of ATc for 24 hours. At least 300 parasites were examined for each condition. Values are means ± SD for three independent experiments. **(C).** The average of TgCentrin1 containing centrosome outer cores per parasite, was quantified in 300 parasites revealing a significant amplification of the centrosome outer core when incenp2i parasites were treated in presence of ATc for 24 hours. Values are means ± SD for three independent experiments. **(D).** Quantification of the number of parasites showing clustered or detached centrosome outer core/kinetochore pairing in two different strains (TATi1-Δku80 and incenp2i) in the presence or absence of ATc for 24 hours. At least 300 parasites were examined for each condition. Values are means ± SD for three independent experiments. **(E).** Intracellular growth of TATi1-Δku80 and Tgincenp2i cultivated in presence or absence of ATc for 24 hours. The percentages of vacuoles containing varying numbers of parasites are represented on the y-axis. Values are means ± SD for three independent experiments.

Figure S12. Hesperadin drug impairs nucleus segregation and the duplication of key subcellular structures associated to mitosis. (A). Quantification of the number of nucleus-deficient parasites treated either with DMSO or Hesperadin drug at 75 nM for 24 hours. The percentage of parasites displaying nucleus segregation defect was determined for at least 300 parasites. The results shown are from three independent experiments. **(B).** Quantification of the number of vacuoles showing nuclei in residual bodies in the presence of DMSO or Hesperadin drug at 75 nM for 24 hours. At least 300 vacuoles were examined for each condition. Values are means ± SD for three independent experiments. **(C and D).** Quantification of the number of parasites showing a stretched centrosome inner core or spindle pole in the presence of DMSO or Hesperadin drug at 75 nM for 24 hours. At least 300 parasites were examined for each condition. Values are means ± SD for three independent experiments. **(E and F).** The average of TgCEP250L1-HA_3 containing centrosomes inner cores or TgEB1-YFP containing spindle poles per parasite, was quantified in 300 parasites revealing a significant reduction of the spindle poles and centrosomes inner cores when parasites were treated in the presence of Hesperadin drug at 75 nM for 24 hours. Values are means ± SD for three independent experiments. **(G and H).** Quantification of the number of parasites showing a stretched kinetochore or centromere in the presence of DMSO or Hesperadin drug at 75 nM for 24 hours. At least 300 parasites were examined for each condition. Values are means ± SD for three independent experiments. **(I).** The average of TgNDC80 containing kinetochores per parasite was quantified in 300 parasites revealing a significant reduction of the kinetochores when parasites were treated in the presence of Hesperadin drug at 75 nM for 24 hours. Values are means ± SD for three independent experiments.

Figure S13. Hesperadin drug abrogates centromere duplication, kinetochore/centromere clustering, proper duplication of the centrosome outer core and centrosome outer

core/kinetochore pairing. (A). The average of TgChromo1 containing centromeres per parasite was quantified in 300 parasites revealing a significant reduction of the centromeres when parasites were treated in the presence of Hesperadin drug at 75 nM for 24 hours. Values are means ± SD for three independent experiments. **(B).** Quantification of the number of parasites showing clustered or detached kinetochore/centromere pairing in the presence of DMSO or Hesperadin drug at 75 nM for 24 hours. At least 300 parasites were examined for each condition. Values are means ± SD for three independent experiments. **(C).** The average of TgCentrin1 containing centrosome outer cores per parasite, was quantified in 300 parasites revealing a significant amplification of the centrosome outer core when parasites were treated in the presence of Hesperadin drug at 75 nM for 24 hours. Values are means ± SD for three independent experiments. **(D).** Quantification of the number of parasites showing clustered or detached centrosome outer core/kinetochore pairing in the presence of DMSO or Hesperadin drug at 75 nM for 24 hours. At least 300 parasites were examined for each condition. Values are means ± SD for three independent experiments.

Figure S14. Overexpression of TgArk1 affects the efficiency of Hesperadin drug on parasite growth. Intracellular growth of ark1WT-Δku80 cultivated in presence of Hesperadin drug at 75 nM and ± shield-1 for 24 hours. The percentages of vacuoles containing varying numbers of parasites are represented on the y-axis. Values are means ± SD for three independent experiments.

Supplementary figure 1

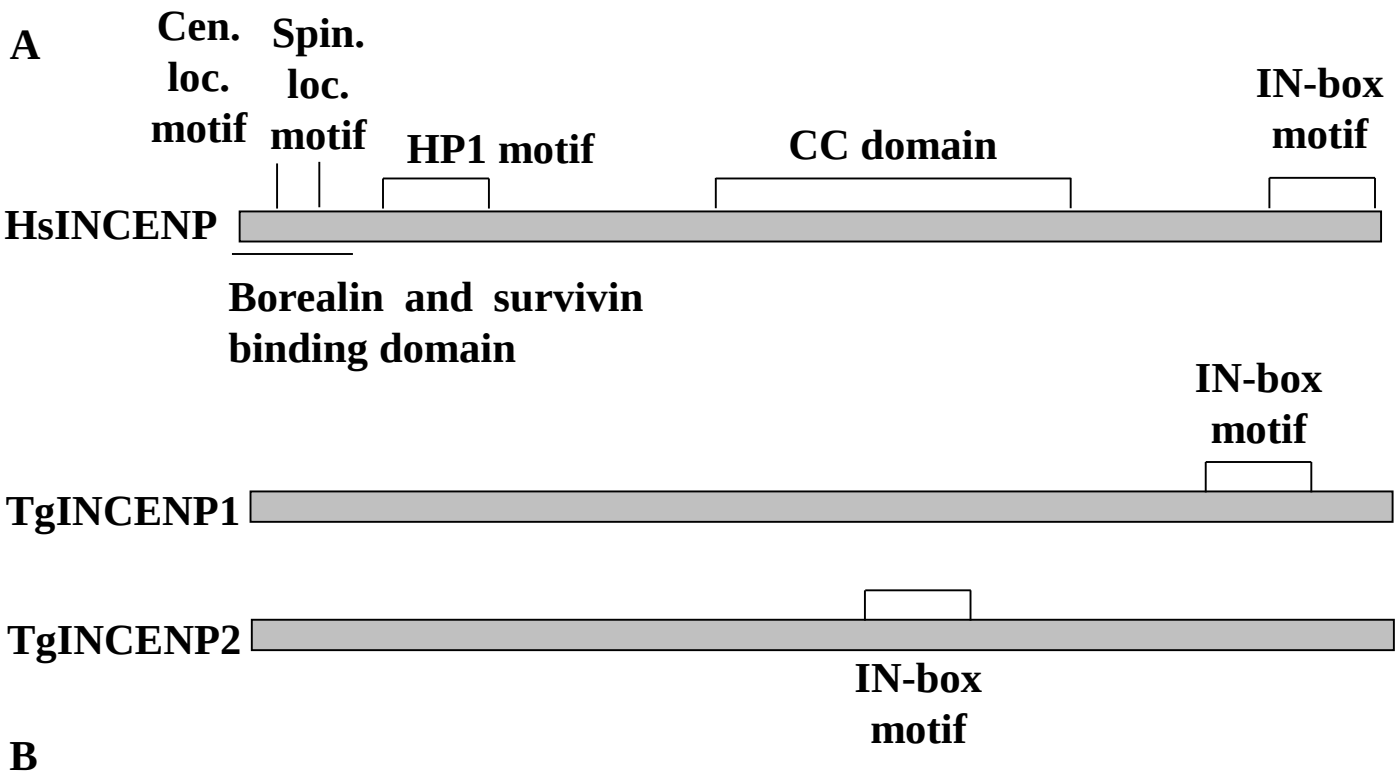

B

```
HsIN-box1   825 DLNSDDSTDDEAHPRKPIPTWA--------------RGTPLSQAIIHQ-YYHPPNLLELF
XlIN-boxA   781 DLNSDDSTDDESQPRKPIPAWA--------------SGNLLTQAIRQQ-YYKPIDVDRMY
TgIN-box1   815 DIPKVDGTYQIGLDMKE-ATWYRPKNPETGMAKPNGKGTAMKKLLEEQERWNP---FSVF
TgIN-box2   654 SLPSVTAALAAGAHPHPCPSWA--------------TREELRAAMSRQDAFNP---FTVF
                    .: .  .:   .   :   :*                    :   : .*  ::*     ::

HsIN-box1   870 GTILP-LDLEDIFKKSKPRYHKRTSSA--------------------------------
XlIN-boxA   826 GTIDS-PKLEELFNKSKPRYFKRTSSA--------------------------------
TgIN-box1   871 GSSLPCVELDDVFDYEV--YSTTAPSARVSHPLFRRLAQFY------------------
TgIN-box2   697 GEAPPELVLSEIYDQRH--YTHVSAQTRASHPVIARLAASHGEAAASRDSEGDRRLQLP
                *       *.::::.     *   : .:
```

C

```
TgArk1  176 LSAPHKMDKVSGSSCASAVNSDLSLVCPLHAYRFCLRDFDFGGFLGDGAHGCVFVARERR
HsARKB   56 ----------------KVMENSSGTPDILTRHFTIDDFEIGRPLGKGKFGNVYLAREKK
XlARKB   72 ----------------EMPSQNTALAEMPKRKFTIDDFDIGRPLGKGKFGNVYLAREKQ
                           : .: :    :   :* : **::*  **.* .* *::***::

TgArk1  236 SGFVCVLKCITKAHLVRGGNEALLKKEVELQAHLKHPHICCMYTWFQTSSAIFLVMEYCL
HsARKB   99 SHFIVALKVLFKSQIEKEGVEHQLRREIEIQAHLHHPNILRLYNYFYDRRRIYLILEYAP
XlARKB  115 NKFIMALKVLFKSQLEKEGVEHQLRREIEIQSHLRHPNILRMYNYFHDRKRIYLMLEFAP
            . *: .** : *::: : * *  *::*:*:*:**:**:*  :*.:*     *:*::*:.
```

Supplementary figure 2

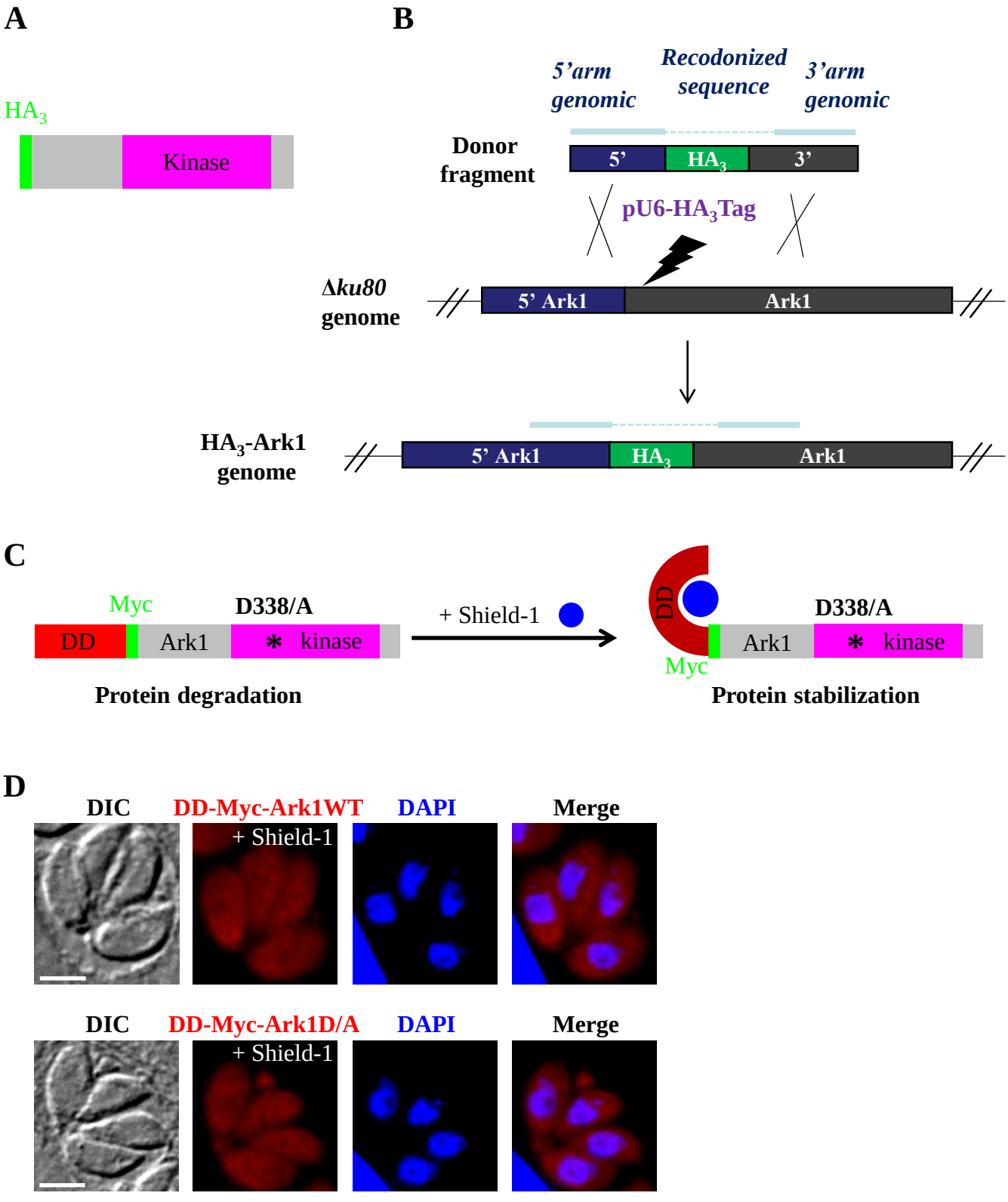

Supplementary figure 3

A

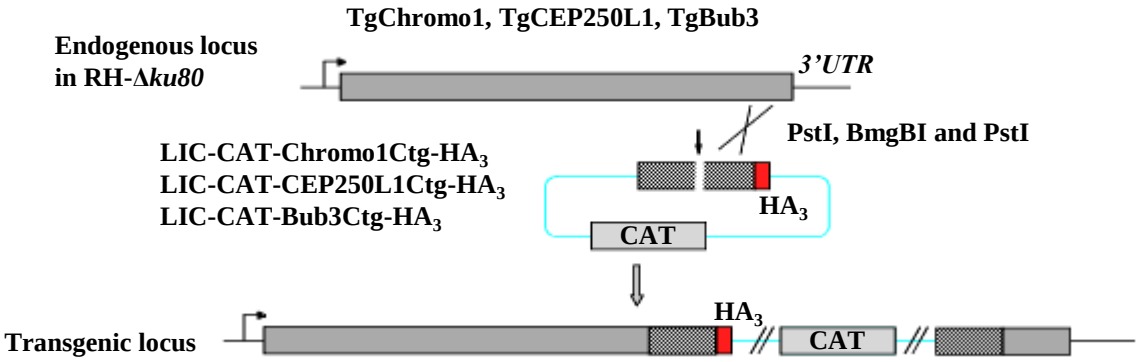

Supplementary figure 4

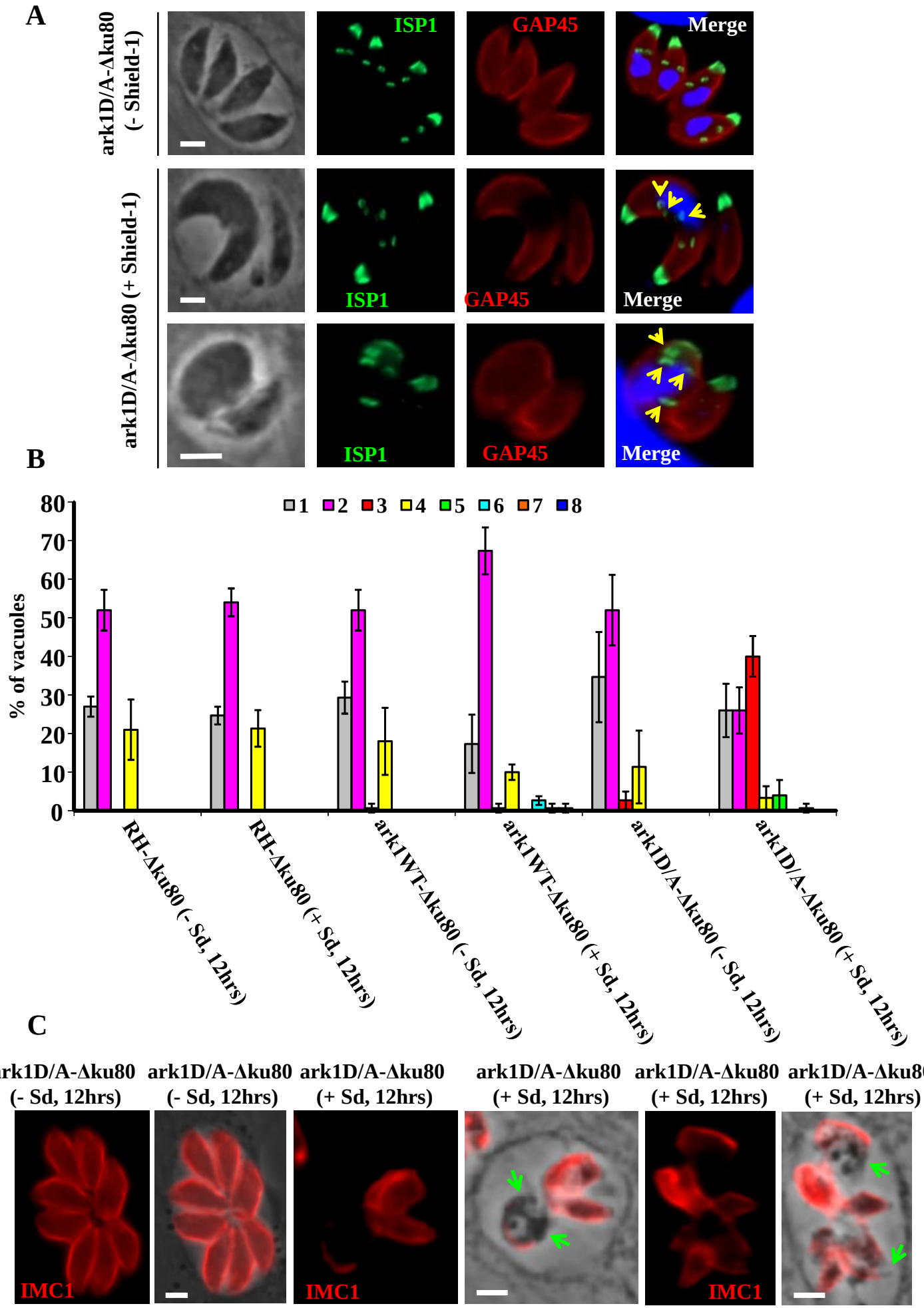

Supplementary figure 5

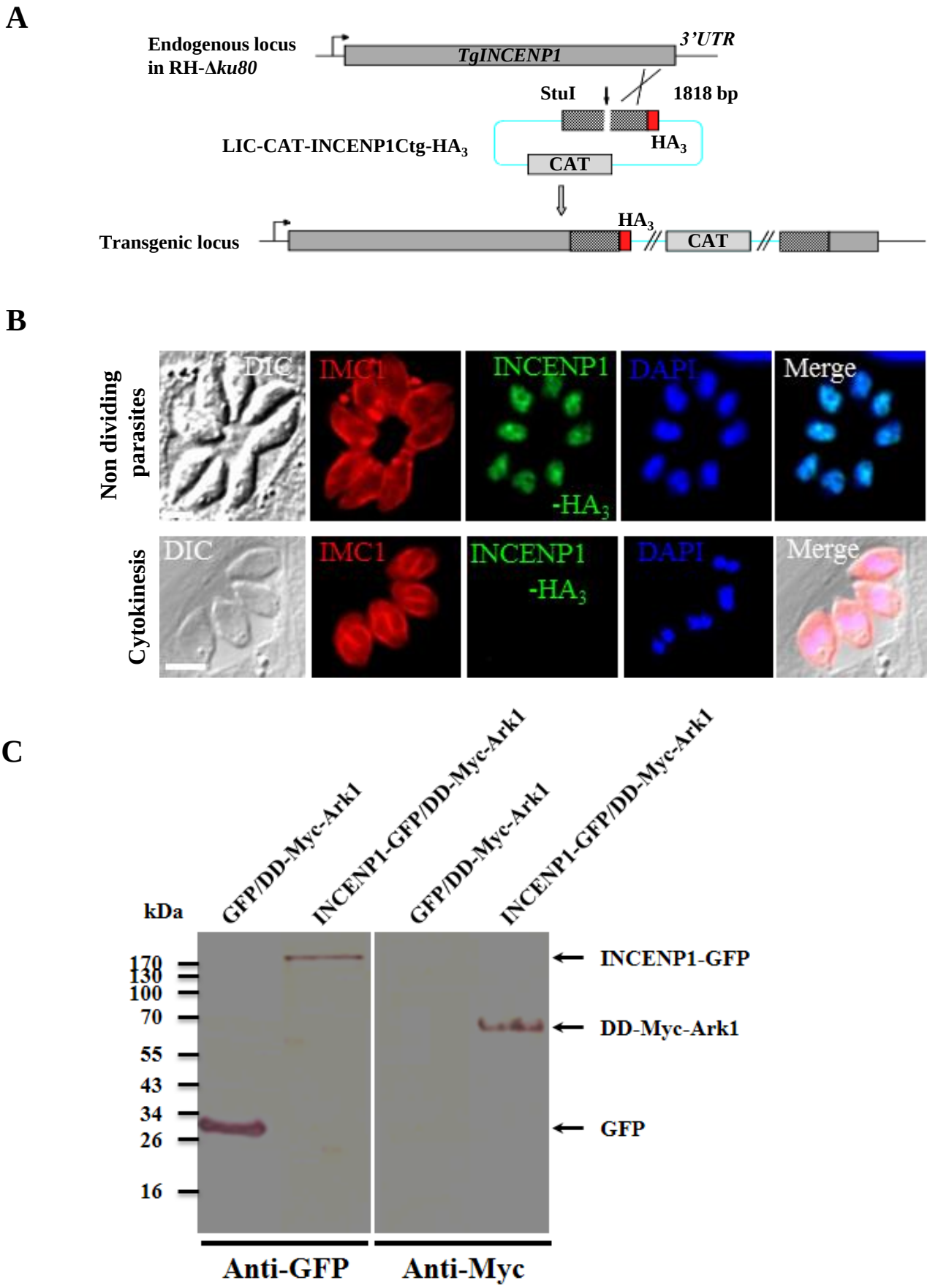

Supplementary figure 6

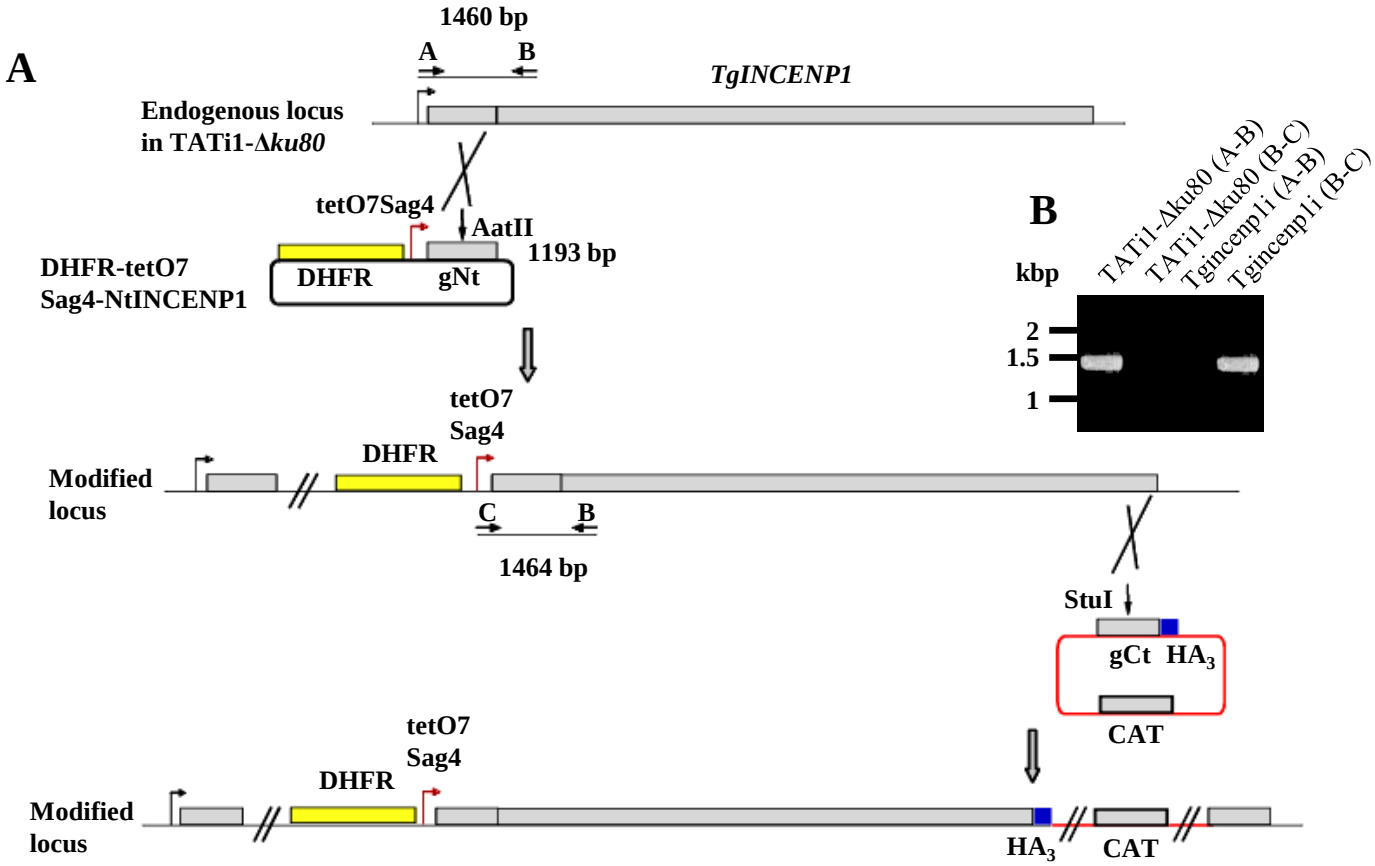

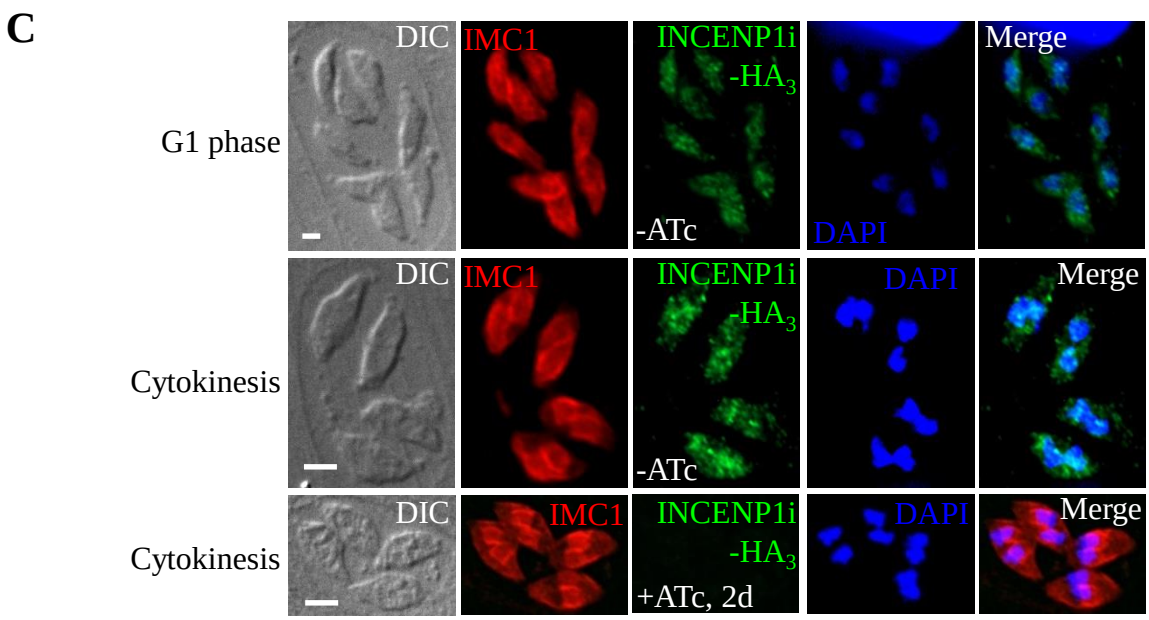

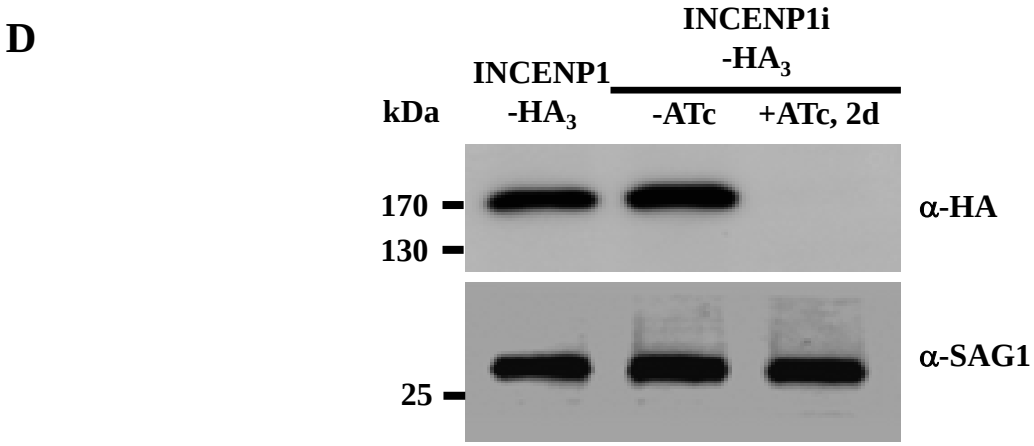

Supplementary figure 7

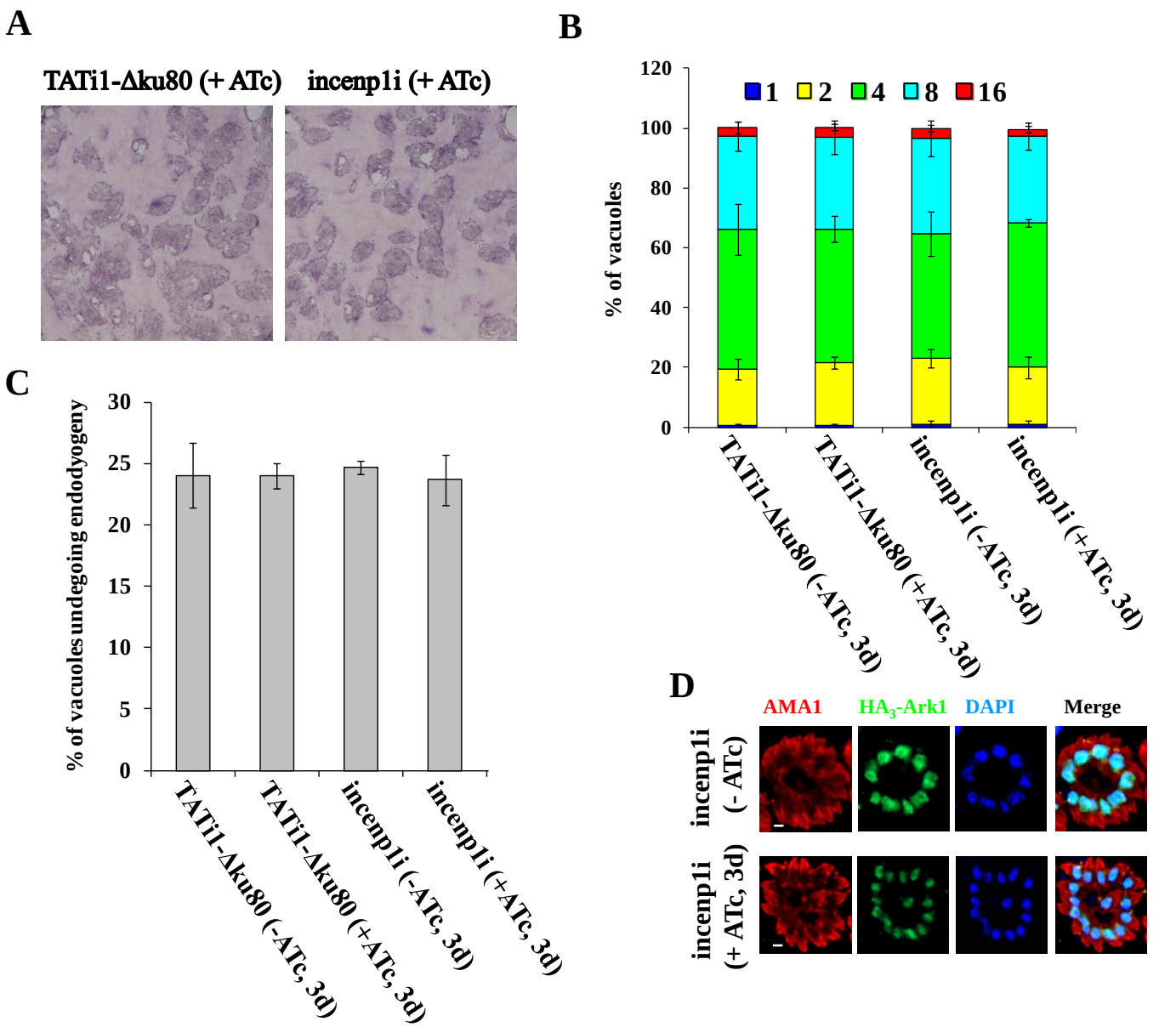

Supplementary figure 8

A

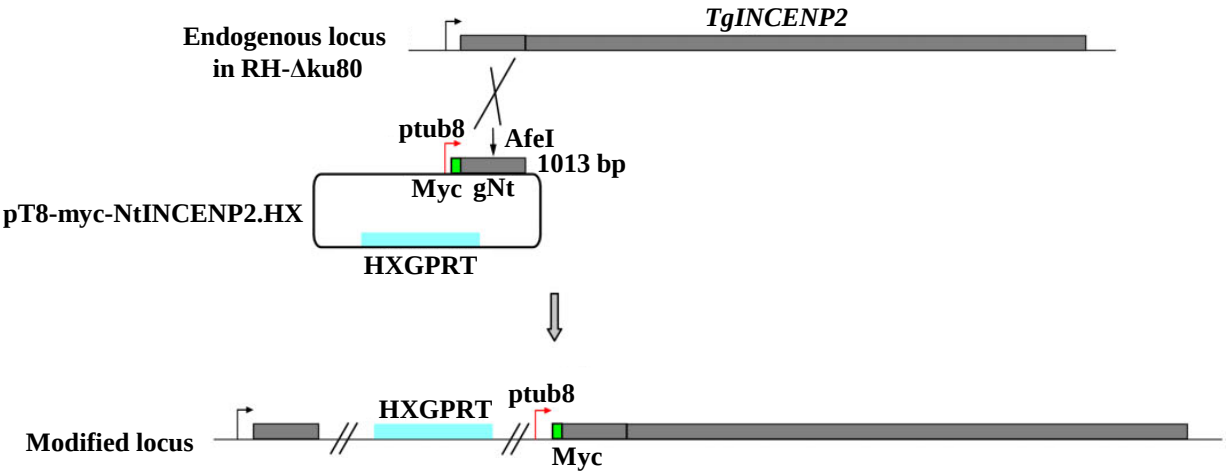

B

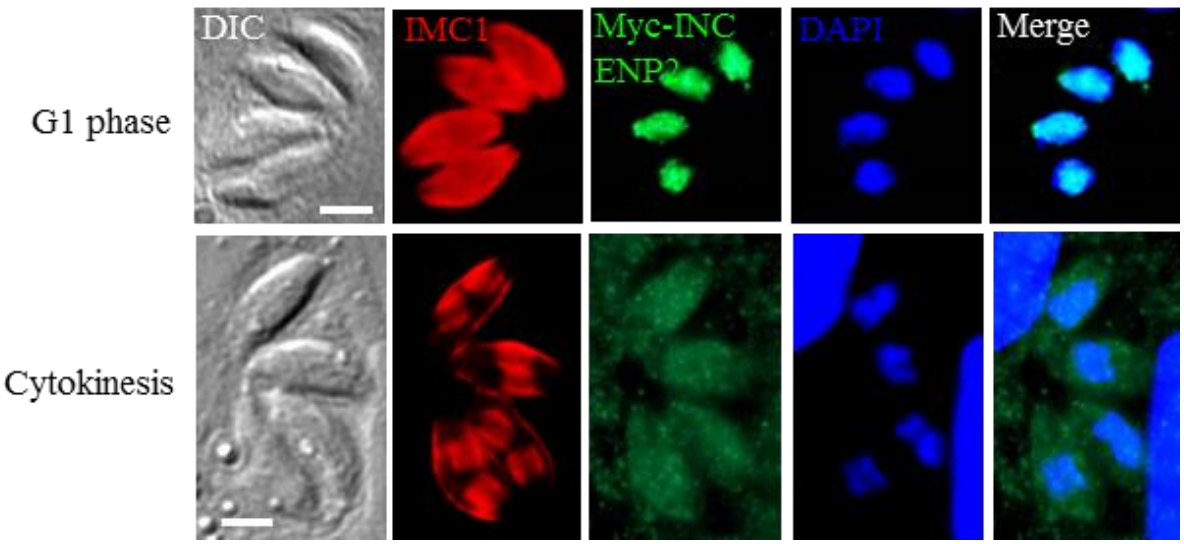

C

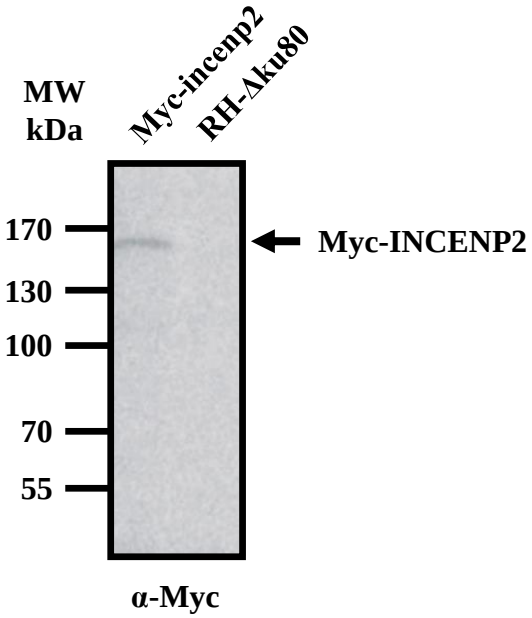

Supplementary figure 9

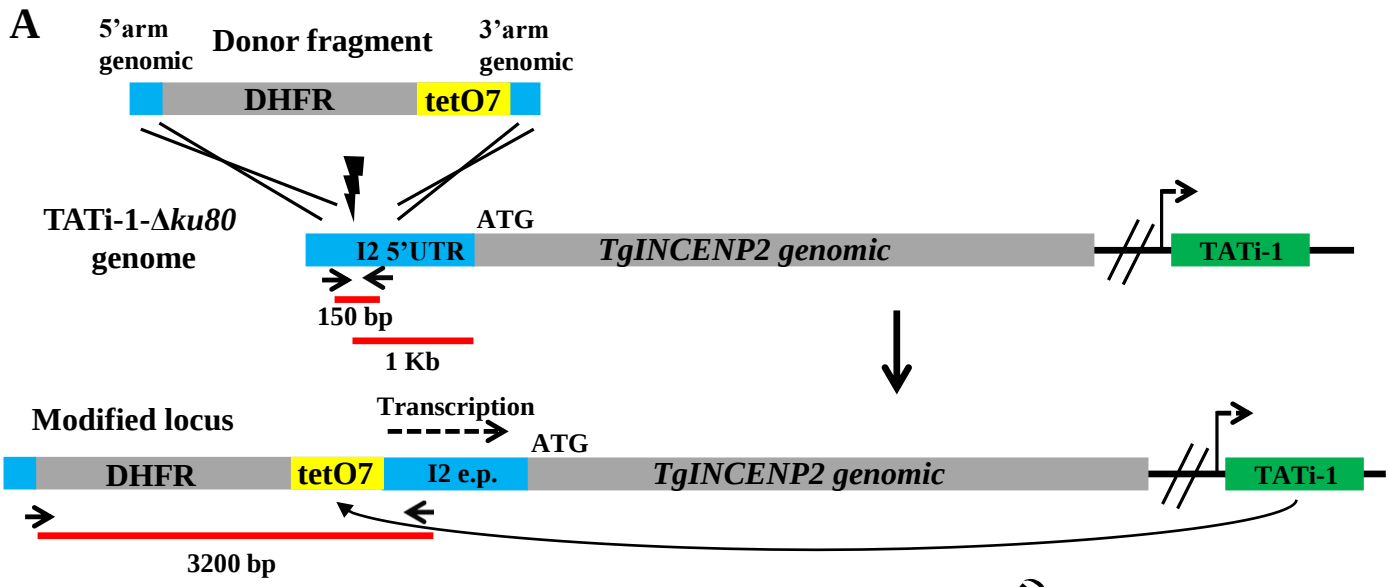

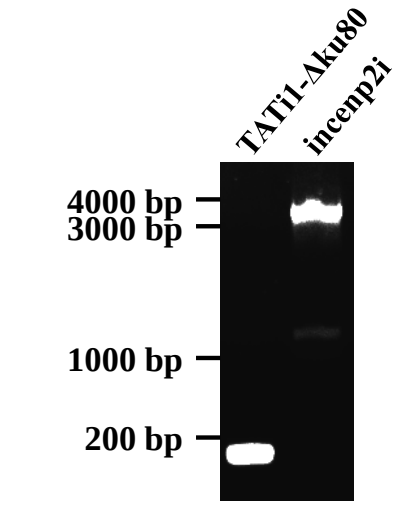

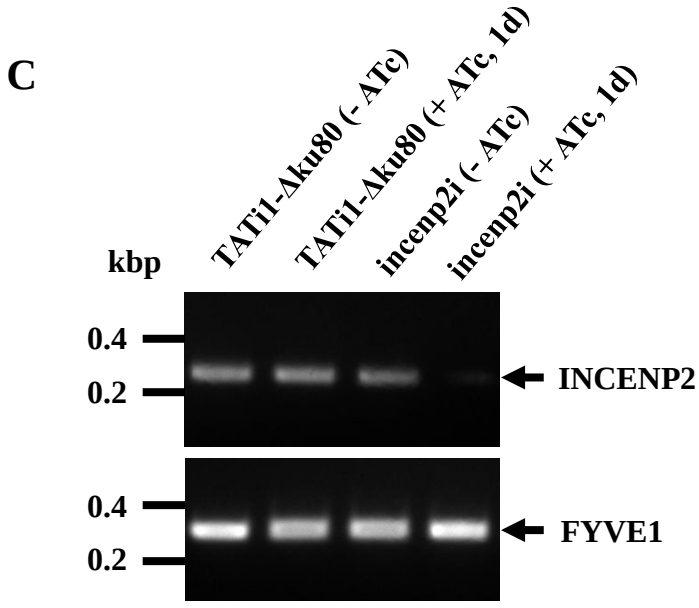

Supplementary figure 10

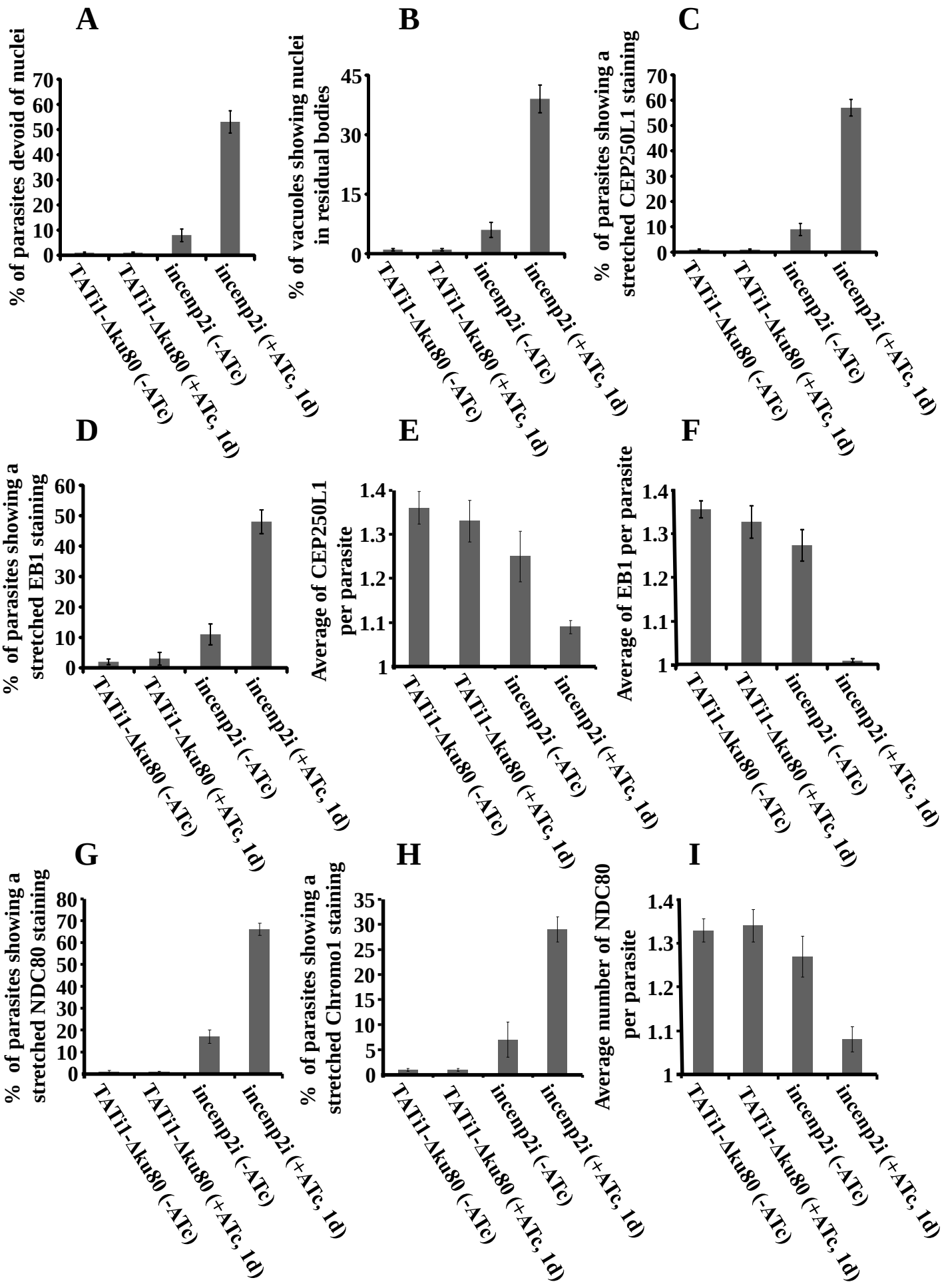

Supplementary figure 11

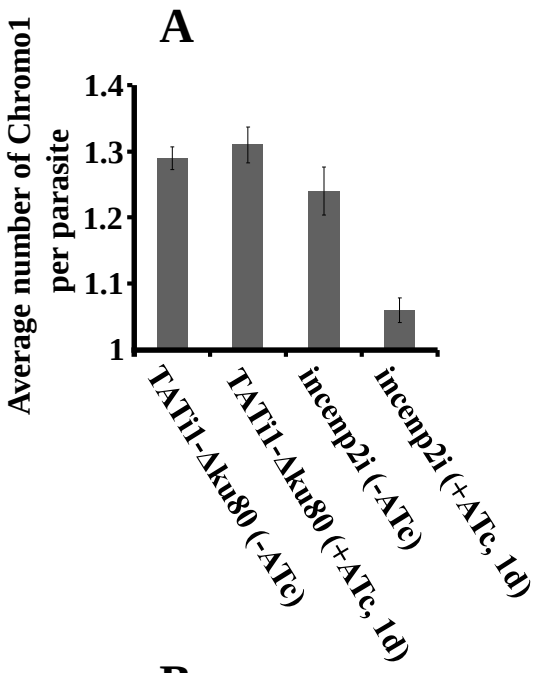

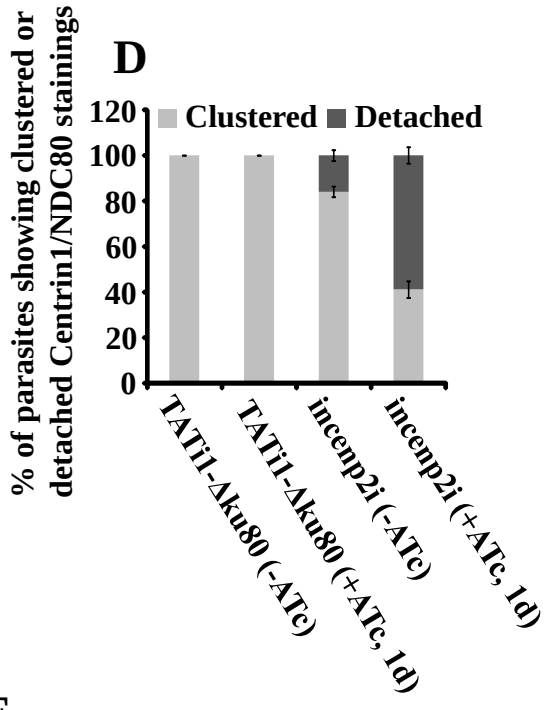

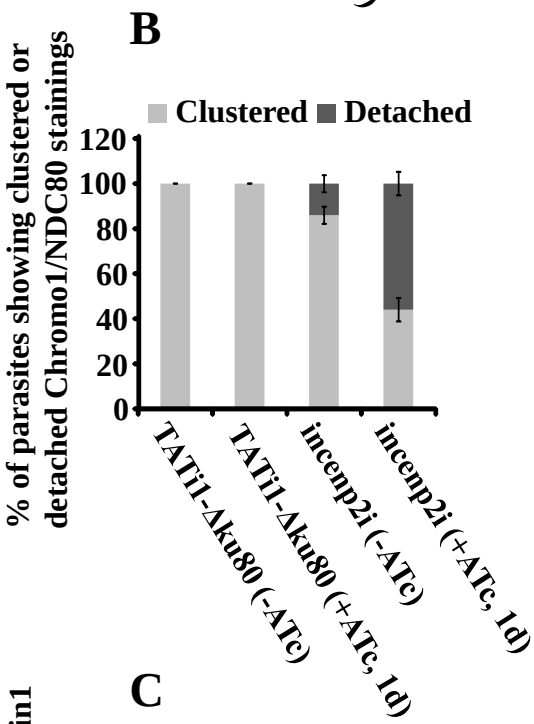

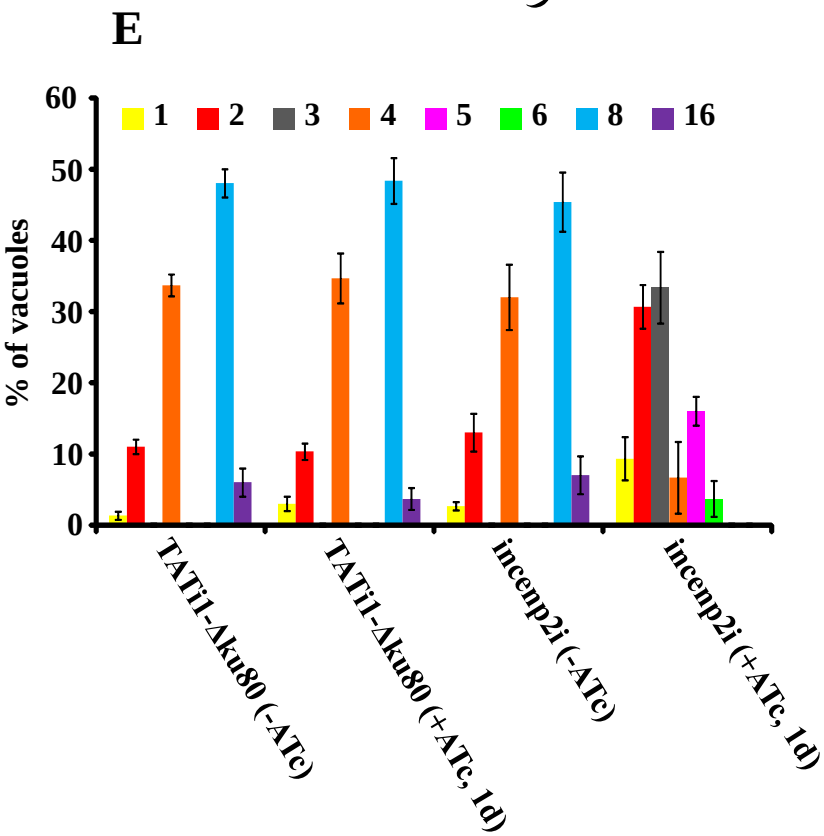

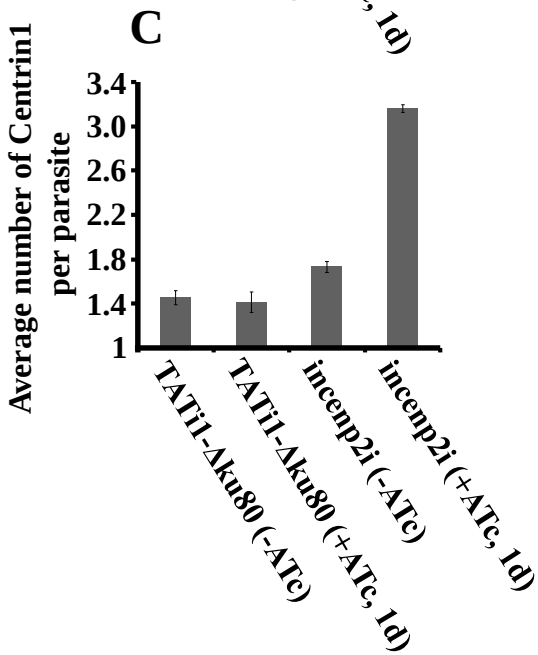

Supplementary figure 12

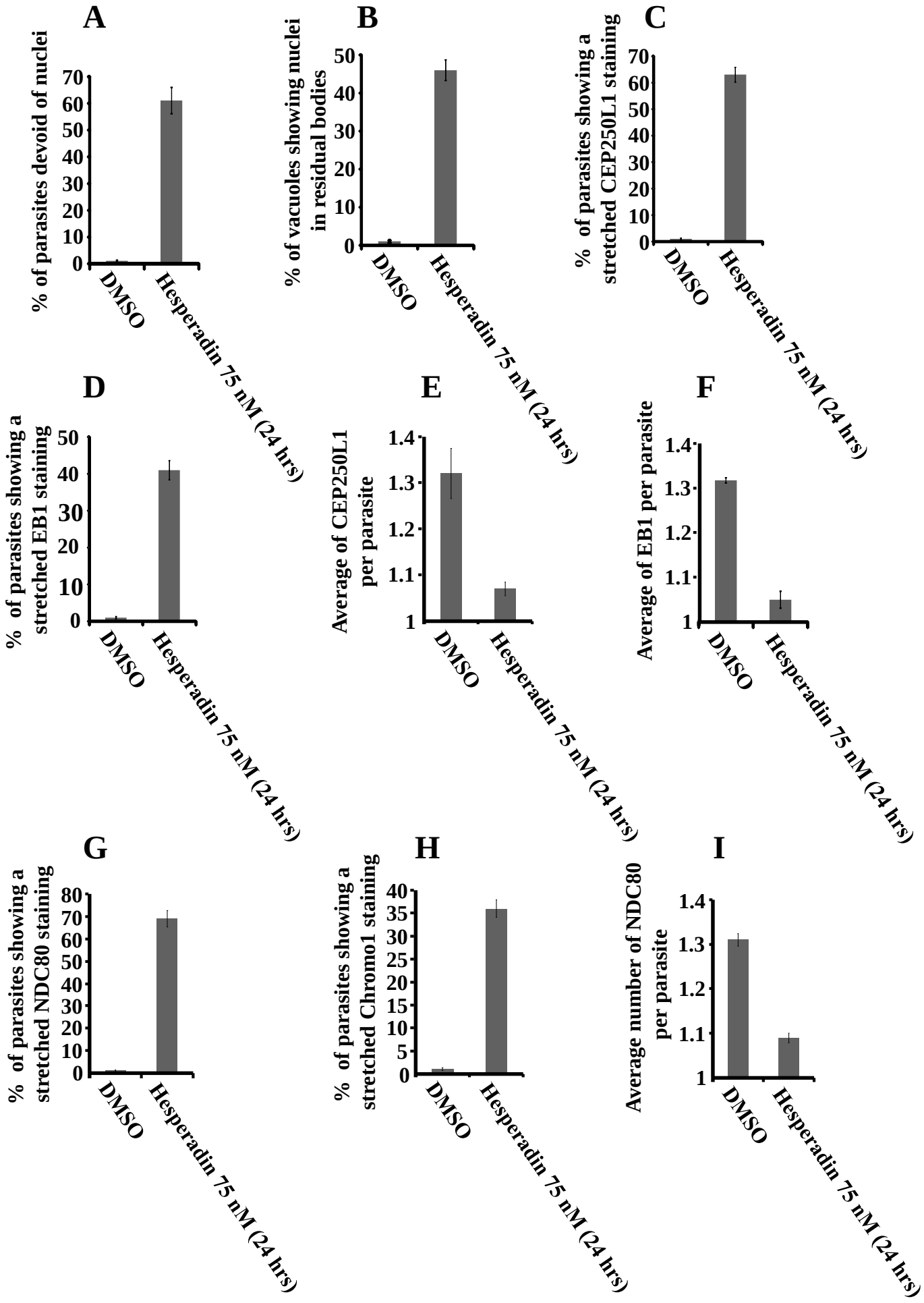

Supplementary figure 13

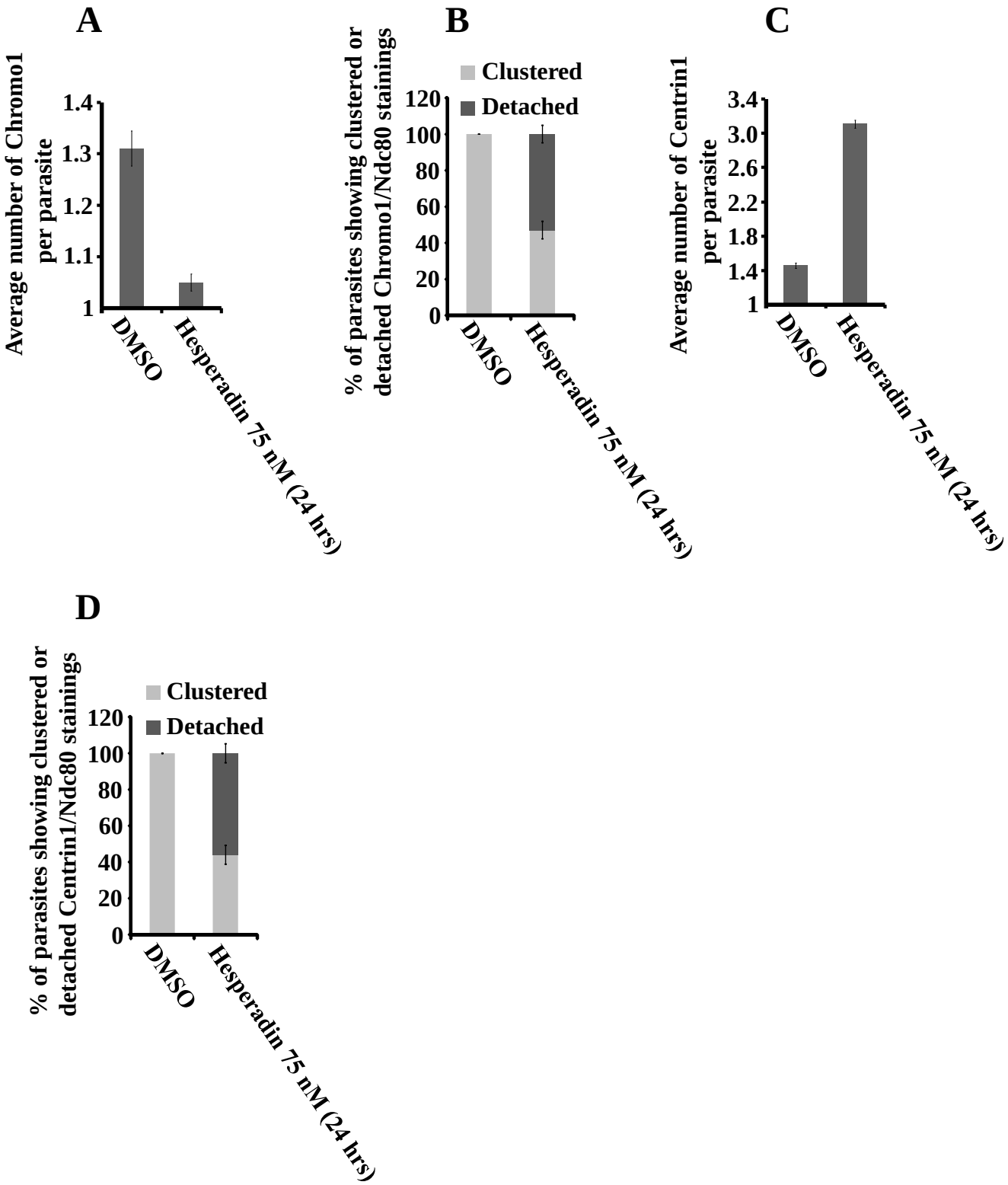

Supplementary figure 14

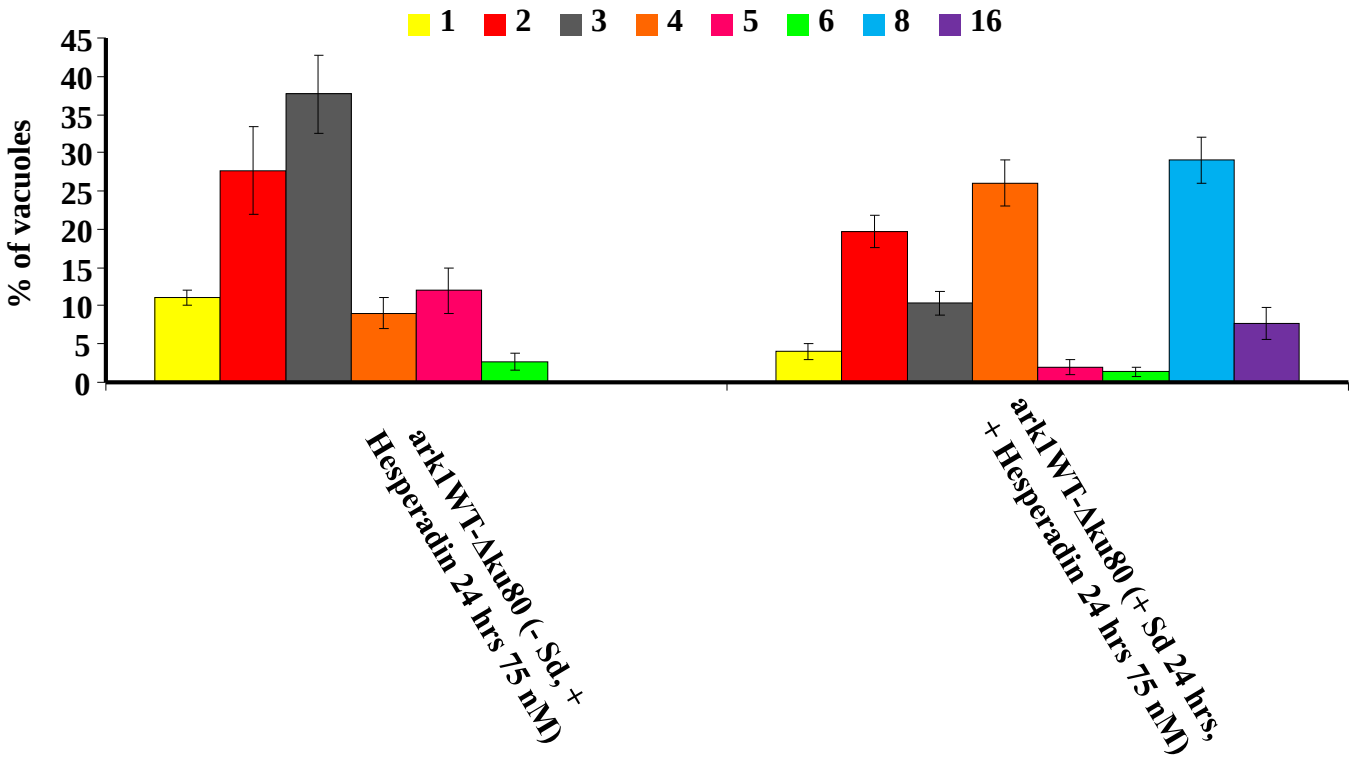

Supplementary table 1: Putative TgArk1 substrates and/or interactants.

Protein annotation	Protein name	Protein accession numbers	Protein molecular weight (kDa)	Number of unique peptide(s)			Motifs/ Domains and putative phosphorylation sites predicted by ToxoDB	Localization
				RH	Myc-Ark1WT	Myc-Ark1D/A		
PEK kinase	TgArk1	TGME49_210280	61	0	24	27	Kinase	Nucleus and cytoplasm
Cytoskeleton associated proteins (putative TgArk1 substrates/interactants)								
Apical cap protein 5 (IMC) (Chen AL, mBio, 2015, e02357-14)	TgAC5	TGME49_235380	65.2	0	2	4	/ S289, S404, S447, S501, S505, S540, and S541	Apical cap of daughter cells
IMC localizing protein 1	TgILP1	TGME49_313380	31.5	0	2	2	/ T184, T187 and T205	Localized to the mature IMC. In dividing parasites, it is preferentially targeted to the daughter buds
IMC19 (Chen AL, mBio, 2015, e02357-14)	TgIMC19	TGME49_217510	42.2	0	1	2	/ /	Posterior IMC
IMC protein (Lorestani A et al., Cytoskeleton, 2012, 1069-1085)		TGME49_230160	16	0	1	2	/ /	IMC
IMC27 (Chen AL et al., CM, 2017, in press)	TgIMC27	TGME49_259630	18.3	0	2	1	/ T27 and T28	Center and base of IMC
Tubulin gamma chain (Suvorova ES et al., PLoS Biology, 2015)	Tgγ-tubulin	TGME49_226870	51.8	0	1	1	Tubulin /	Centrosome
Microtubule associated protein SPM2 (Tran JQ, EC, 2012, 206-216)	TgSPM2	TGME49_286590	40	1	2	3	/ S32, S40, T98 and T103	Middle region of the subpellicular microtubules
Actin-related protein 4 (chromosome segregation and mitosis) (Suvorova ES, MBP, 2012, 7-16)		TGME49_258050	60.4	1	3	3	Actin /	Nucleus
Factors involved in: DNA replication, DNA repair, chromatin assembly, chromosome segregation, genome integrity and regulation of gene expression (putative TgArk1 substrates/interactants)								
DNA replication licensing factor MCM5	TgMCM5	TGME49_243920	88.2	0	2	7	MCM T93	ND
DNA replication licensing factor Mcm7		TGME49_237220	97	1	2	5	AAA-ATPases	ND

							S182, S631, S633, S661, S855 and S858	
XPG N-terminal domain-containing protein (nuclease involved in DNA replication, repair, and recombination)		TGME49_212250	87	0	1	3	/ S408	ND
WD domain, G-beta repeat-containing protein (chromatin assembly factor 1, histone transcription regulator 1)		TGME49_294250	56	0	0	3	WD40 S145, S146 and S348	ND
Histone H3.3 (regulation of gene expression)		TGME49_218260	15.4	0	1	1	Histone H3 /	Nucleus
Acetyltransferase (catalyzes N-acetyltransferase reactions)		TGME49_259070	51.9	0	1	1	/ S237	ND
Nuclear pore proteins and factors involved in material transport into the nucleus (putative TgArk1 substrates/interactants)								
Nuclear pore complex protein NUP54	TgNup37	TGME49_248500	37.6	0	1	3	/ /	ND
Putative nucleoporin	TgNup503	TGME49_269290	503.4	0	1	1	/ S535, S1097, S1105, S1106, S1108, S1111, S1399, S1566, S1569, S1669, S2400, S2408, S2410, S2422, T2424, S2440, T2443, S2444	ND
Nuclear pore associated protein (Courjol Flavie et al., Cell Mol Life Sci, 2017, 2107-2125)	TgNup115	TGME49_219120	116	1	5	6	Zinc finger S645	Nuclear membrane
Cell cycle regulators (putative TgArk1 substrates/interactants)								
Cyclin2 related protein (interacts with TgCrk2 and regulate progression through the tachyzoite G1 phase) (Alvarez CA and Suvorova ES, PLoS Pathogens, 2017)	TgPHO80	TGME49_267580	95	0	1	1	Cyclin S18, T202, S204, S301, S304, S325, S335, S342, S354, S500, T506, S509, S526, S528, S529, T530, S875	Cytoplasmic

Supplementary table 2: list of primers used in this study.

Number	5'→3' sequence	Restriction site	Plasmid F (sense), R (antisense)
1	AAGTTGATGTTGGCATCCAAGTGCGGG	-	Guide to generate HA_3-Ark1
2	AAAACCCGCACTTGGATGCCAACATCA	-	Guide to generate HA_3-Ark1
3	AAACTTCCAATCTCAACGGC	-	Donor DNA to generate HA_3-Ark1
4	ATACGAAGCCGGCGCCTCCAGT	-	Donor DNA to generate HA_3-Ark1
5	cctgcaggccATGTTGGCATCCAAGTGCGGCGG	SbfI	DD-Myc-Ark1 WT vector (F)
6	ttaattaaTTAGCAGCACGTCGGCCGAGG	PacI	DD-Myc-Ark1 WT vector (R)
7	CGCATTGCCCACCTTGCCATAAAACCCGAAAACGTTCTCG	-	DD-Myc-Ark1D/A vector (F)
8	CGAGAACGTTTTCGGGTTTTATGGCAAGGTGGGCAATGCG	-	DD-Myc-Ark1D/A vector (R)
9	TACTTCCAATCCAATTTAAtgcgaagactccgagaggctgcatgc	-	LIC-CAT-Chromo1Ctg-HA_3 (F)
10	tcctccacttccaattttagcGCCAGCGACACAAGAGAACACTGG	-	LIC-CAT-Chromo1Ctg-HA_3 (R)
11	TACTTCCAATCCAATTTAAtgcGAGGACGACGGAAAG CAGGCGAC	-	LIC-CAT-Cep250L1Ctg-HA_3 (F)
12	tcctccacttccaattttagcTCGCCCCGAAAGCGACGACTTTC	-	LIC-CAT-Cep250L1Ctg-HA_3 (R)
13	TACTTCCAATCCAATTTAAtgcgtgttccgagtcatcttatctccatac	-	LIC-CAT-Bub3Ctg-HA_3 (F)
14	tcctccacttccaattttagcTGCCTGCAATGCCTTGGGCCTC	-	LIC-CAT-Bub3Ctg-HA_3 (R)
15	TACTTCCAATCCAATTTAAtgcGACACAGGAGCATTCTGTTC ACCCG	-	LIC-CAT-INCENP1Ctg-HA_3 (F)
16	tcctccacttccaattttagcGGAAAGAACATCTCTCCTGAATTTGGAAC	-	LIC-CAT-INCENP1Ctg-HA_3 (R)
17	TACTTCCAATCCAATTTAAtgcGACACAGGAGCATTCTGTTC ACCCG	-	LIC-CAT-INCENP1Ctg-GFP (F)
18	tcctccacttccaattttagcGGAAAGAACATCTCTCCTGAATTTGGAAC	-	LIC-CAT-INCENP1Ctg-GFP (R)
19	AGATCTATGCCGAGCTCTCGGGGTAAG	BglII	DHFR-tetO7Sag4-Ntincenp1 (F)
20	GCGGCCGCGACGCTAGCTTCGAGGTTATCTGTTG	NotI	DHFR-tetO7Sag4-Ntincenp1 (R)
21	gaaaagctagtcagtcgcatgcggag (A)	-	To check integration incenp1i (F)
22	CTTCTGATTGCTGCAGTTCAAAGCGTG (B)	-	To check integration incenp1i (R)
23	CGGATCATTTGAAAACATCGTGAGGCTGG (C)	-	To check integration incenp1i (F)
24	ATGCATATGTCTAACTCTCTTGGGTCGTTTCTTCTG	NsiI	pT8myc-NtINCENP2.HX (F)
25	ttaaTTAAGCCGATGAGAGATACCCTCCCC	PacI	pT8myc-NtINCENP2.HX (R)
26	AAGTTGCCCAATTAGCGTTCTCTCAGG	-	Guide to generate incenp2i
27	AAAACCTGAGAGAACGCTAATTGGGCA	-	Guide to generate incenp2i
28	GACGTGGAAGTCACACAGCTGGCCTCTGAGTTTACCACTC CCTATCAGTG	-	Donor DNA to generate incenp2i
29	GACGTGGAAGTCACACAGCTGGCCTCTGATTATCGA TACCGTCGACCTC	-	Donor DNA to generate incenp2i
30	TTTTCCGCGTCATCTGACCA	-	To check integration incenp2i (F)
31	CAGTTGCTTTGTCAAAGAGG	-	To check integration incenp2i (R)
32	GAGGGCCTATCCCTGGAATACAC	-	*INCENP2* gene, RT-PCR (F)
33	GTGAGGTTTGCATGCCCCTGAGG	-	*INCENP2* gene, RT-PCR (R)
34	GGATCCATGAGCGAGAACGAAAATCC	-	*FYVE1* gene, RT-PCR (F)
35	AAGCTTAGGTGTGAGAGGACGCACG	-	*FYVE1* gene, RT-PCR (R)
36	AAGTTGAAGTTCCCAAAATACTGCAG	-	Guide 1 to disrupt *KU80* gene
37	AAAACTGCAGTATTTTGGGAACTTCA	-	Guide 1 to disrupt *KU80* gene
38	AAGTTGCTTCAGAGAAAAATGCCGTCG	-	Guide 2 to disrupt *KU80* gene
39	AAAACGACGGCATTTTTCTCTGAAGCA	-	Guide 2 to disrupt *KU80* gene
40	TGTTTCTACTTGCAAGGCGGAAGTTCCCAACGACGGC CAGTGAATTGTAA	-	Donor DNA to disrupt *KU80* gene
41	AAGAGCAACCACTCCCGTTTTGTCAAAGACACAGCA CGAAACCTTGCATT	-	Donor DNA to disrupt *KU80* gene